

Experimental Study of the Interaction between Terahertz Radiation from the Novosibirsk Free-Electron Laser and Water Aerosol

G. N. Kulipanov^a, A. A. Lisenko^b, G. G. Matvienko^b, V. K. Oshlakov^b, V. V. Kubarev^a,
E. N. Chesnokov^c, and S. V. Babchenko^b

^a Budker Institute of Nuclear Physics, Siberian Branch, Russian Academy of Sciences,
pr. Akademika Lavrent'eva 11, Novosibirsk, 630090 Russia

^b V.E. Zuev Institute of Atmospheric Optics, Siberian Branch, Russian Academy of Sciences,
pl. Akademika Zueva 1, Tomsk, 634055 Russia

^c Institute of Chemical Kinetics and Combustion, Siberian Branch, Russian Academy of Sciences,
ul. Institutskaya 3, Novosibirsk, 630090 Russia

e-mail: G.N.Kulipanov@inp.nsk.su, Lisenko@iao.ru, mgg@iao.ru, ovk@iao.ru,
chesnok@kinetics.nsc.ru, bsvetlana@sibmail.com

Received August 8, 2014

Abstract—Interactions of high-power terahertz radiation from the Novosibirsk free-electron laser at a wavelength of 130 μm in an atmospheric window with a model aerosol cloud with a known droplet size distribution function has been studied experimentally for the first time. The experimental data are compared with theoretical calculation results obtained from solution of the lidar equation for conditions of the experiment.

Keywords: THz radiation, free-electron laser, remote sensing

DOI: 10.1134/S1024856015020062

INTRODUCTION

The significant advance in the THz radiation generation and reception (0.3–10 THz frequencies corresponding to $\lambda = 1\text{ mm}–30\text{ }\mu\text{m}$) currently achieved promotes intense development of different systems for remote monitoring of the atmosphere. New-generation millimeter and submillimeter radiometers have been designed for satellite monitoring systems of the phase composition of stratospheric ice crystal clouds and related radiation processes; they are capable of operating at frequencies of up to 3 THz [1, 2]. This frequency coverage ensures high sensitivity for a wide size range of cloud particles, since THz wavelengths are comparable with diameters of large cloud particles [3, 4].

The development of remote sensing of the lower atmosphere, which is inaccessible for satellite measurements, with the aim to study spatiotemporal variability of the water content of the atmosphere, phase composition of low clouds, fogs, and precipitation, and other problems also requires extension of the frequency range of active remote sensing instruments. We should note that, so far, there are no THz radiation sources suitable for active remote sensing. Therefore, the interest from specialists in environmental lidar sensing in the Novosibirsk free-electron laser (FEL) is clear. First, the pulse and the average spectral radiation powers of this laser are a world record and will apparently remain so in the near future ($P_p \sim 0.7\text{ MW}$, $P_{av} \sim 0.5\text{ kW}$) [5]. No one currently available THz

radiation source has a power sufficient for implementation of the above applications in the lower atmosphere. Second, a wide range of continuous wavelength tuning of the FEL allows implementation of multifrequency sensing of microphysical aerosol parameters, i.e., there is a possibility of selecting sensing wavelengths in atmospheric windows in the whole FEL operation range from 7 to 235 μm , which are of high information content for a wide class of remote sensing problems. The 7–30 μm range, which corresponds to the currently designed 3rd stage of the FEL, has been studied quite well, while there is a series of questions concerning the 30–235 μm range, which corresponds to the 1st and 2nd currently operating stages of the FEL: the questions are connected with the lack of experimental studies of both atmospheric transmission and THz radiation interaction with water aerosols.

In general, interaction of THz radiation with water droplet aerosols has been studied theoretically quite well, but has not been practically confirmed so far. Filling this gap is the aim of our experimental study.

EXPERIMENTAL TECHNIQUE

A test bench has been designed for the experiment on interaction of THz radiation with water droplet aerosols; it consists of radiation source (FEL) (1), optomechanical modulator (2), Newtonian telescope (3), aerosol cloud (4), radiation detector (5),

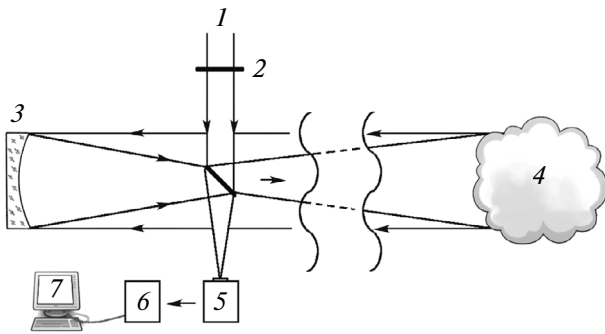


Fig. 1. Layout of the experiment.

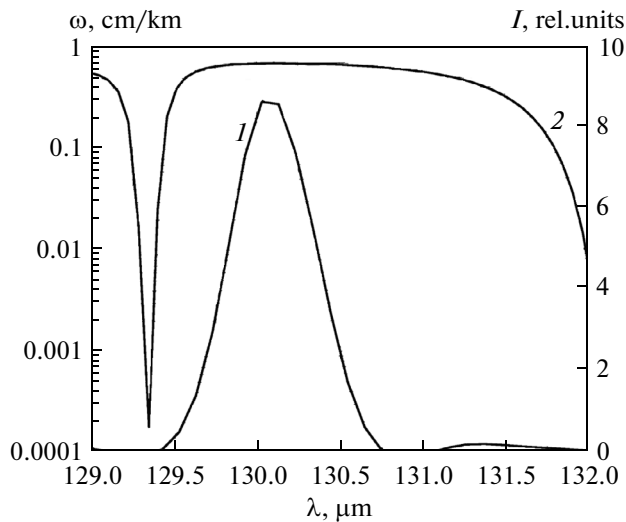


Fig. 2. Novosibirsk FEL 130- μm radiation spectrum (I) in an atmospheric window calculated at a distance of 20 m at the specific water vapor content $w = 0.12$ cm/km (2).

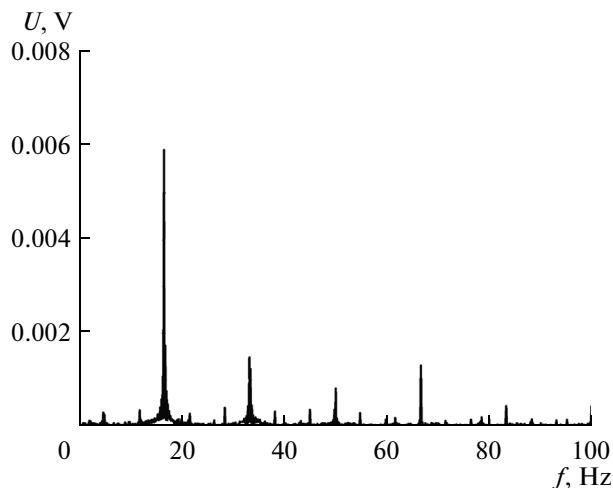


Fig. 3. Backscattering signal from a water aerosol cloud recorded with the GC-1P optoacoustic detector with a modulation frequency of 17 Hz. Neighboring peaks form the external thermal background modulated by frequencies multiple of electric circuit frequency (50 Hz) and other frequencies connected with mechanical oscillations falling in the detector sensitivity range.

electronic unit for data acquisition and processing (6), and computer (7) (Fig. 1).

FEL radiation at a wavelength of 130 μm had the following parameters: the degree of linear polarization $>99.6\%$, diffraction beam, divergence angle $\theta = 4$ mrad, beam FWHM diameter on the telescope $d_0 = 3$ cm, pulse repetition rate $f = 5.6$ MHz, average power $P_{av} = 100$ W, pulse length $\tau = 100$ ps, $P_p = 0.2$ MW. The radiation spectrum in an atmospheric window recorded with the Bruker IFS 66 v/S spectrometer is shown in Fig. 2.

The window transmission T was calculated on the basis of data from the JPL Submillimeter Catalogue, which includes data on 916 lines of water molecules in the ground vibrational state and 55983 absorption lines of vibrationally excited water molecules over a distance of 10 m at the specific water vapor content $w = 0.12$ cm/km.

To detect backscattering signals, a GC-1P optoacoustic detector (Golay Cell, Tydex [6]) was used; it relates to the class of low-selective uncooled detectors capable of recording low-energy signals of up to 10^{-5} J in the wavelength range from 0.3 μm to 6–8 mm. The main feature of the use of this detector is the need to use a modulator that interrupts the radiation flux measured. An operating frequency ($f_r = 17$ Hz) was selected on the basis of the fact that the 10–25 Hz range is an optimal frequency range, where the detector sensitivity is the highest. Key power parameters of the GC-1P optoacoustic detector are the following at a modulation frequency of 17 Hz and the entrance window diameter $d = 5$ mm: the optical responsivity $W = 8.7 \times 10^4$ V/W, the noise-equivalent power $NEP = 1.1 \times 10^{-10}$ W/Hz $^{1/2}$, the time constant $t = 36$ ms, and the detectivity $D^* = 3.9 \times 10^9$ Hz $^{1/2}$ /(W cm). The detectivity characterizes the signal-to-noise ratio (S/N) while 1-W radiation falls on the receiving aperture of the detector; it is calculated by the equation

$$D^* = \frac{S/N \sqrt{\Delta f}}{P \sqrt{A}}, \quad (1)$$

where S is the detector output signal, N is the receiver noise, P is the power at the detector entrance, A is the receiving aperture area, cm 2 , and Δf is the noise band width, Hz. The noise equivalent power $NEP = \sqrt{A}/D^*$, W/Hz $^{1/2}$.

The experiment consisted in recording the radiation modulated in the optoacoustic modulator and scattered by an aerosol cloud located at a short (up to 10 m) path. The scattered radiation was collected by the Newtonian telescope with a mirror of $S_r = 0.07$ m 2 in area and focused to the entrance of the optoacoustic detector. A signal from the head transmitter was transferred into the electronic module for data acquisition and processing.

Figure 3 exemplifies a recorded backscattering signal from the aerosol cloud at a distance of 3 m. The plot is a FFT spectrum (Fourier transform) of an input signal. The frequency is plotted along the abscissa. The power spectral density of the input signal in RMS (root mean square) is plotted along the ordinate; it is connected with the square root of the frequency band width. The backscattering signal has a peak with amplitude of 0.0058 V at a frequency of 17 Hz. If the optical sensitivity of the detector is known, one can calculate P and S/N from Eq. (1). In our case, $S/N = 8$. Noise signals were detected at frequencies multiple of 50 Hz during the recording, which form the thermal background; this can be explained by equipment operation in a 50-Hz circuit and at other frequencies connected with mechanical oscillations falling in the detector sensitivity range.

SIMULATION

To simulate the experiment, let us estimate the S/N ratio accounting the FEL radiation parameters, optical circuit of the detection, parameters of the GC-1P optoacoustic detector, and optical parameters of the model cloud and atmosphere. The S/N ratio can be estimated from the equation [7, 8]:

$$S/N = \frac{P_s}{\sqrt{2\Delta f(P_s + P_b) \frac{2hc}{\lambda\eta} + NEP^2\Delta f}}, \quad (2)$$

where η is the detector quantum efficiency, h is the Planck constant, and c is the speed of light.

The power of a lidar echo signal from the aerosol cloud is defined as

$$P_s = P_p \frac{c\tau}{2} K(r)G(r)\beta_\pi(r) \left(\frac{S_r}{r^2}\right) T_a^2. \quad (3)$$

Here P_p is the FEL peak power, $K(r)$ is the instrument constant, τ is the pulse length, S_r is the area of the receiving antenna, $G(r)$ is the geometry factor, $\beta_\pi(r)$ is the volume backscattering coefficient per unit solid angle, and T_a is the atmospheric and aerosol cloud transmittance, which is defined by the Bouguer–Lambert–Beer law at the given wavelength:

$$T_a = \exp\left(-\int_0^R [\gamma_m(\lambda, r) + \gamma_a(\lambda, r)] dr\right), \quad (4)$$

where r is the distance, γ_m and γ_a are the atmospheric and aerosol cloud radiation attenuation coefficients.

In addition to the FEL radiation and detector parameters, a variation in the index of molecular absorption by atmospheric water vapor is also considered in the numerical experiment. The molecular scattering, obeying the λ^{-4} law, does not play a significant role in the THz range and can be neglected. The absorption indices α at a wavelength of 130 μm are shown in Fig. 4 for different specific water vapor con-

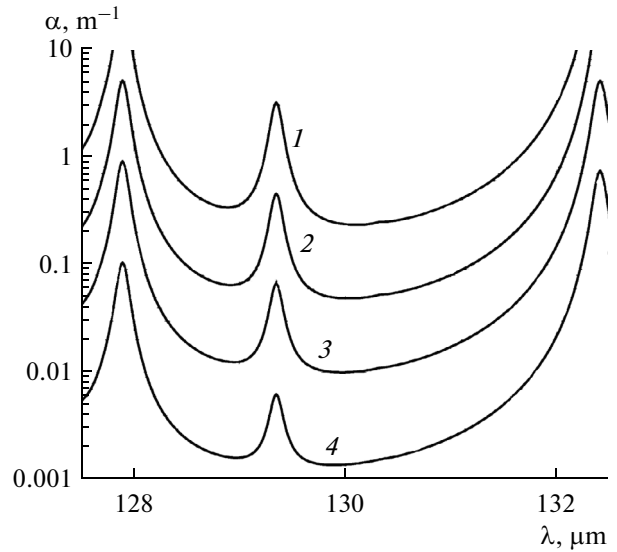


Fig. 4. Absorption in an atmospheric window centered at 130 μm as a function of the specific water vapor content $w = 0.6$ (1), 0.12 (2), 0.02 (3), and 0.03 cm/km (4).

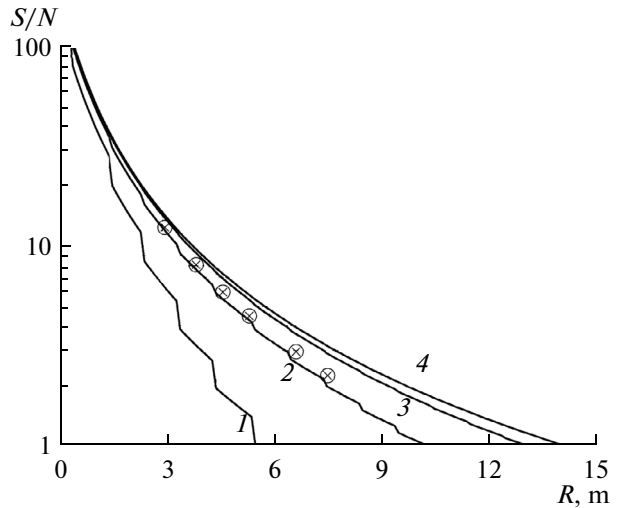


Fig. 5. Comparison of experimental and calculated S/N at a wavelength of 130 μm : $w = 0.6$ (1), 0.12 (2), 0.02 (3), and 0.003 cm/km (4).

tent w . The scattering by the water aerosol cloud is described by the Mie theory, which is valid for scattering by large particles, comparable in size or larger than the wavelength, and small particles, which are much smaller than the wavelength. A cloud model described by the lognormal size distribution of droplets with a modal radius of 2 μm was chosen for calculations of optical parameters of the interaction between 130- μm FEL radiation and the aerosol cloud. The Mie calculations provided the following values of the optical coefficients of the interaction: the attenuation coefficient $\gamma_a = 1.31 \times 10^{-6} \text{ m}^{-1}$ and the backscattering coefficient $\beta_\pi = 1.03 \times 10^{-8} \text{ m}^{-1}$. These parameters were used in our calculations.

Figure 5 shows the S/N ratio (solid curves) calculated for different water vapor content along the sensing path; the circles show experimental values of S/N measured at different distances to the aerosol cloud. The measurements fall well on the curve that corresponds to a water vapor content of 0.12 cm/km, which is close to real experimental conditions.

CONCLUSIONS

Experimental measurements and numerical simulation of the backscattering signal from an aerosol cloud of droplets of 2 μm in modal radius at a wavelength of 130 μm have shown a good qualitative agreement between the results. This indicates that an increase in the backscattering signal by orders of magnitude may be expected in an aerosol cloud of droplets comparable in size with the wavelength. These experiments are planned to be carried out at the Novosibirsk free-electron laser in the near future.

REFERENCES

1. P. H. Siegel, "THz instruments for space," *IEEE Trans. Antennas Propag.* **55** (11), 2957–2965 (2007).
2. P. Racette, R. F. Adler, J. R. Wang, A. J. Gasiewski, D. M. Jackson, and D. S. Zacharias, "An airborne millimeter-wave imaging radiometer for cloud, precipitation, and atmospheric water vapor studies," *J. Appl. Ocean. Technol.* **13** (3), 610–619 (1996).
3. D. L. Wu, H. M. Pickett, and N. J. Livesey, "Aura MLS THz observations of global cirrus near the tropopause," *Geophys. Res. Lett.* **35**, L15803 (2008).
4. J. Mendrok, P. Baron, and Y. Kasai, "Studying the potential of Terahertz radiation for deriving ice cloud microphysical information," *Proc. SPIE—Int. Soc. Opt. Eng.* **7107** (2008).
5. G. N. Kulipanov, N. G. Gavrilov, B. A. Knyazev, E. . Kolobanov, V. V. Kotenkov, V. V. Kubarev, A. N. Matveenko, L. E. Medvedev, S. V. Miginsky, L. A. Mironenko, V. K. Ovchar, V. M. Popik, T. V. Salikova, M. A. Scheglov, S. S. Serednyakov, O. A. Shevchenko, A. N. Skrinsky, V. G. Tcheskidov, and N. A. Vinokurov, "Research highlights from the Novosibirsk 400 W average power THz FEL," *Terahertz Sci. Technol.* **1** (2), 107–125 (2008).
6. <http://www.tydex.ru>
7. R. M. Measures, *Laser Remote Sensing. Fundamentals and Applications* (Wiley, New York, 1984).
8. M. V. Ivashchenko and I. V. Sherstov, "Operating range of a differential-absorption lidar based on CO₂ lasers," *Kvant. Electron.* **30** (8), 747–752 (2000).

Translated by O. Ponomareva